

NbNi_{2.38}Te₃, a New Metal-Rich Niobium Telluride with a "Stuffed" TaFe_{1+x}Te₃ Structure

Jörg Neuhausen, E. Wolfgang Finckh, and Wolfgang Tremel*

Institut für Anorganische Chemie und Analytische Chemie der Johannes Gutenberg-Universität Mainz, Becherweg 24, D-55128 Mainz, Germany

Received March 24, 1995

In the last few decades early transition metal chalcogenides received the attention of many scientists, both physicists and chemists, because of their diverse and unusual physical and chemical properties. Superconductivity¹ and charge density wave (CDW) behavior² as well as anisotropic electrical and optical properties³ have been observed for many of these materials. These phenomena originate in the electronic structure of this class of compounds, which is characterized by incompletely filled conduction bands. Most of these materials have low dimensional structures leading to a rich intercalation chemistry,⁴ and potential applications in battery systems or as lubricants.

Originally, almost all studies were concentrated on sulfides and selenides, whereas the tellurides were neglected. Only the last few years saw an uprise in early transition metal telluride chemistry. This led to the discovery of numerous new binary and ternary phases with unique structures. For example, Ta₅Te₅,⁵ MM'Te₅ (M = Nb, Ta; M' = Ni, Pd, Pt),⁶ Ta_{1.09}Fe_{2.39}Te₄,⁷ M₄M'Te₄ (M = Nb, Ta; M' = Si, Cr, Fe, Co),⁸ M₃M'Te₆ (M = Nb, Ta; M' = Si, Ge),⁹ Ta₄BTe₈,¹⁰ and MGeTe₄ (M = Zr, Hf)¹¹ all have no counterparts among the sulfides and selenides. The origin of the different behaviour of sulfides and selenides on one hand and tellurides on the other hand is not yet clear. Neither packing considerations nor electronic reasoning based on band structure calculations on the extended Hückel level allows for a reliable differentiation between the tellurides and their lighter homologues. Indeed, we have recently

Table 1. Crystallographic Data for NbNi_{2.38}Te₃

NbNi _{2.38} Te ₃	fw = 615.6 g mol ⁻¹
a = 7.405(2) Å	space group P2 ₁ /m (No. 11)
b = 3.7623(5) Å	T = 298 K
c = 10.005(2) Å	λ = 0.71073 Å
β = 105.70(2)°	ρ _{calc.} = 7.619 g/cm ³
V = 268.34(10) Å ³	μ = 26.160 mm ⁻¹
Z = 2	R ^a = 0.025
	R _w ^b = 0.031

$$^a R = \sum ||F_o| - |F_c|| / \sum |F_o|. \quad ^b R_w = [\sum (w(|F_o| - |F_c|)^2) / \sum (w|F_o|)^2]^{1/2}.$$

Table 2. Atomic Coordinates and Equivalent Isotropic Thermal Parameters^a (Å²) for NbNi_{2.38}Te₃

atom	Wyckoff site	x	y	z	U _{eq}
Nb	2c	0.70807(8)	1/4	0.20502(6)	0.0108(1)
Ni(1)	2e	0.0996(1)	1/4	0.58824(8)	0.0126(2)
Ni(2)	2c	0.5468(1)	1/4	0.92849(8)	0.0114(2)
Ni(3) ^b	2e	0.7157(3)	1/4	0.5044(3)	0.0152(7)
Te(1)	2c	0.08252(6)	1/4	0.32876(4)	0.0130(1)
Te(2)	2e	0.21765(6)	1/4	0.99465(4)	0.0116(1)
Te(3)	2e	0.46571(6)	1/4	0.66100(4)	0.0122(1)

^a Equivalent isotropic U defined as one-third of the trace of the orthogonalized U_{ij} tensor. ^b Site occupancy 0.382(6).

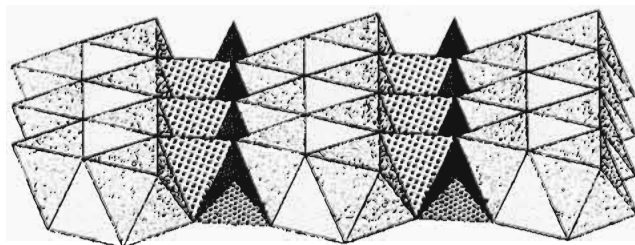


Figure 1. Polyhedral representation of a NbNi₂Te₃-layer (NbTe₆-octahedra: random dot pattern, NiTe₄-tetrahedra: crossed (Ni(1)), tetrahedral sites of type B: regular dot pattern Ni(2)). Ni(3) atoms are situated in the square hollows formed by three Ni(1)Te₄-tetrahedra and one NbTe₆-octahedron.

succeeded in the synthesis of Ta₂Ni₃Se₅,¹² the first ternary tantalum selenide with an existing Te-analog, Ta₂Ni₃Te₅.¹³ This result shows that further experimental work is needed to obtain a satisfactory understanding of the differences and similarities in sulfide/selenide and telluride chemistry. Here we report the synthesis, structure and electrical properties of the new metal-rich telluride NbNi_{2.38}Te₃.

Experimental Section

Synthesis. NbNi_{2.38}Te₃ was synthesized by heating the elements—Nb powder (Starck, 99.99%), Ni powder (Alfa, 99.9%) and Te powder (Merck 99.9%)—in a ratio of Nb:Ni:Te = 1:2:2 in a sealed evacuated silica tube (length approx. 20 cm, diameter 18 mm). Doubly sublimated iodine (approx. 2 mg/cm³) was added as a mineralizer. The tube was placed into a two-zone furnace with a temperature gradient from 850 to 700 °C with the charge at the hot end. After 14 days long flat crystals (single phase material, EDAX on several crystals: Nb, Ni, Te) showing metallic luster were formed at the cold end of the tube (yield approximately 60%). Elemental analysis yielded a bulk composition of Nb_{0.99(3)}Ni_{2.39(4)}Te_{3.00(2)}. X-ray structure refinements on several single crystals from batches with different starting compositions showed variations of the sample composition according to a formula NbNi_{2+x}Te₃ (x ≈ 0.2–0.4).

X-ray Powder Diffraction. The samples were examined using an Enraf-Nonius Fr 552 vacuum Guinier camera with monochromated

- Yvon, K. *Curr. Top. Mater. Sci.* **1979**, *3*, 53. Chevrel, R. In *Superconductor Materials Science*; Flomer, S., Schwartz, B. B., Eds.; Plenum: New York, 1981; Chapter 10.
- Wilson, J. A.; DiSalvo, F. J.; Mahajan, S. *Adv. Phys.* **1975**, *24*, 117. Rouxel, J. Ed.; *Crystal Chemistry and Properties of Materials with Quasi One-Dimensional Structures*; Reidel: Dordrecht, The Netherlands, 1986. Monceau, P., Ed. *Electronic Properties of Inorganic Quasi One-Dimensional Compounds, Part 1 and 2*; Reidel: Dordrecht, The Netherlands, 1985. Kamimura, H., Ed. *Theoretical Aspects of Band Structures and Electronic Properties of Pseudo One-Dimensional Solids*; Reidel: Dordrecht, The Netherlands, 1985.
- Wilson, J. A.; Yoffe, A. D. *Adv. Phys.* **1969**, *18*, 193.
- Whittingham, M. S.; Jacobson, A. J., Eds. *Intercalation Chemistry*; Academic Press: New York, 1982. Friend, R. H.; Yoffe, A. D. *Adv. Phys.* **1987**, *36*, 1. Rouxel, J.; Brec, R. *Annu. Rev. Mater. Sci.* **1986**, *16*, 137.
- Conrad, M.; Harbrecht, B. Personal communication, 1991.
- Liimatta, E. W.; Ibers, J. A. *J. Solid State Chem.* **1987**, *71*, 384. Liimatta, E. W.; Ibers, J. A. *J. Solid State Chem.* **1988**, *77*, 141. Liimatta, E. W.; Ibers, J. A. *J. Solid State Chem.* **1989**, *78*, 7. Mar, A.; Ibers, J. A. *J. Solid State Chem.* **1991**, *92*, 352.
- Neuhausen, J.; Tremel, W. *J. Alloys Compd.* **1994**, *204*, 215.
- Badding, M. E.; DiSalvo, F. J. *Inorg. Chem.* **1990**, *29*, 3952. Ahn, K.; Hughbanks, T.; Rathnayaka, K. D. D.; Naugle, D. G. *Chem. Mater.* **1994**, *6*, 418. Neuhausen, J.; Finckh, E. W.; Tremel, W. *Chem. Ber.*, in press.
- Li, J.; Caroll, P. J. *Mater. Res. Bull.* **1992**, *27*, 1073. Monconduit, L.; Evain, M.; Boucher, F.; Brec, R.; Rouxel, J. *Z. Anorg. Allg. Chem.* **1992**, *616*, 177. Canadell, E.; Monconduit, L.; Evain, R.; Brec, R.; Rouxel, J.; Whangbo, M.-H. *Inorg. Chem.* **1993**, *32*, 10. Li, J.; Badding, M. E.; DiSalvo, F. J. *J. Alloys Compd.* **1993**, *184*, 257.
- Kleinke, H.; Tremel, W. *Angew. Chem.*, submitted for publication.
- Mar, A.; Ibers, J. A. *J. Am. Chem. Soc.* **1993**, *115*, 3227.

- Neuhausen, J.; Tremel, W. *Proceedings: Soft Chemistry Routes to New Materials*, Trans Tech Publications: Aedermannsdorf, Switzerland, 1994; Vols. 152–153, p 383.
- Tremel, W. *Angew. Chem.* **1991**, *103*, 900; *Angew. Chem., Int. Ed. Engl.* **1991**, *30*, 840.

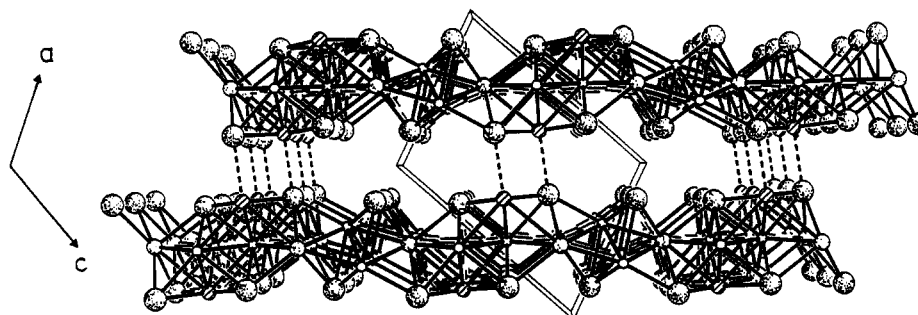


Figure 2. Projection of the structure of $\text{NbNi}_{2.38}\text{Te}_3$ along $[010]$ (Te, large, heavily dotted circles; Nb, medium, light dotted circles; Ni(1), small open circles; Ni(2), dotted circles; Ni(3), hatched circles).

Table 3. Important Interatomic Distances (Å) for $\text{NbNi}_{2.38}\text{Te}_3$

Nb–Ni(1)	2.872(1) (2×)	Ni(1)–Ni(1)	2.725(1) (2×)
Nb–Ni(2)	2.742(1) (2×)	Ni(1)–Ni(3)	2.738(3)
Nb–Ni(3)	2.980(3)	Ni(1)–Ni(3)	2.637(2) (2×)
Nb–Te(1)	2.714(1)	Ni(1)–Te(1)	2.579(1) (2×)
Nb–Te(2)	2.903(1) (2×)	Ni(1)–Te(1)	2.565(1)
Nb–Te(3)	2.815(1) (2×)	Ni(1)–Te(3)	2.610(1)
		Ni(3)–Ni(1)	2.738(3)
Ni(2)–Ni(2)	2.570(1) (2×)	Ni(3)–Ni(1)	2.637(2) (2×)
Ni(2)–Te(2)	2.539(1) (2×)	Ni(3)–Te(1)	2.685(2) (2×)
Ni(2)–Te(2)	2.693(1)	Ni(3)–Te(3)	2.622(2) (2×)
Ni(2)–Te(3)	2.579(1)	Ni(3)–Te(3)	2.730(3)

$\text{CuK}\alpha_1$ radiation ($\lambda = 1.54056 \text{ \AA}$) and quartz as an internal standard. The experimental powder patterns were in almost perfect agreement with those calculated from the single-crystal data using the program Lazy-Pulverix.¹⁴

Structure Determination. Preliminary checks of crystal quality and Laue symmetry using film methods indicated monoclinic symmetry. Overexposed Weissenberg photographs gave no indications for superstructure formation. Single crystal studies were carried out on a flat needle-shaped crystal (dimensions $0.005 \times 0.02 \times 0.2 \text{ mm}$) using a Syntex P2₁ four-circle diffractometer equipped with graphite monochromator (Mo $\text{K}\alpha$ radiation, $\lambda = 0.71073 \text{ \AA}$) and a scintillation counter. Relevant crystallographic data are listed in Table 1. All calculations were performed with the SHELXTL/PC program system.¹⁵ A total of 2595 reflections were collected ($4^\circ \leq 2\theta \leq 70^\circ$; $\pm h, +k, \pm l$), of which 1322 were unique ($R_{\text{int}} = 0.033$) and 1130 considered observed ($F > 4.0\sigma(F)$). Conventional atomic scattering factors were used and anomalous dispersion corrections were applied.¹⁶ The processed data were empirically corrected for absorption effects using the program XEMP. Systematic extinctions led to the possible space groups $P2_1/m$ (No. 11) and $P2_1$ (No. 4). The choice of the centrosymmetric space group $P2_1/m$ (rather than $P2_1$) was proved to be correct based on the refinement results. Direct methods yielded the positions of three Te atoms, one Nb atom, and two Ni atoms. The additional, partially occupied Ni site was located from subsequent difference electron density maps. Anisotropic refinement with a free occupancy parameter for the partially occupied Ni site resulted in $R = 0.025$ ($R_w = 0.031$) and a composition of $\text{NbNi}_{2.382(6)}\text{Te}_3$ in excellent agreement with the analytical data. Atomic parameters and important interatomic distances are compiled in Tables 2 and 3. Further information on the crystal structure analysis is available as supplementary material.

Resistivity Measurements. A flat needle-shaped crystal (dimensions $0.03 \times 0.5 \times 3 \text{ mm}$) was mounted on a sample holder and four gold leads were attached along the needle axis using silver epoxy. The resistivity was measured as a function of temperature from 290 to 5 K and reverse at increments of 2 K. The absolute values of resistivity are only approximate due to difficulties in measuring the crystal dimensions accurately.

Results and Discussion

The structure of $\text{NbNi}_{2.38}\text{Te}_3$ is built up by layers of composition NbNi_2Te_3 which are linked by Ni atoms located at the layer surfaces. Figure 1 gives a polyhedral representation of a NbNi_2Te_3 layer, whereas a projection of the complete structure along the crystallographic b -axis is shown in Figure 2. The layers are stacked along $[10\bar{1}]$. Each slab consists of $[\text{Nb}_2\text{Te}_6]$ double chains of edge sharing octahedra which are interconnected by $[\text{Ni}_2\text{Te}_4]$ double chains of edge-sharing tetrahedra to give layers of composition $[(\text{Nb}_2\text{Te}_2\text{Te}_{4/2})(\text{Ni}_2\text{Te}_{4/2})] \equiv \text{NbNiTe}_3$. In fact, the NbTe_6 octahedra are heavily distorted ($d_{\text{Nb-Te}(1)} = 2.714(1) \text{ \AA}$; $d_{\text{Nb-Te}(2)} = 2.903(1) \text{ \AA}$ (2×); $d_{\text{Nb-Te}(3)} = 2.815(1) \text{ \AA}$ (2×); $d_{\text{Nb-Te}(2)} = 3.672(1) \text{ \AA}$) resulting in a 5-fold rather than 6-fold Te-coordination of niobium. Thus, the idealized picture of NbTe_6 octahedra is chemically not correct, but it facilitates discussion and clearly shows the structural relationship between $\text{NbNi}_{2.38}\text{Te}_3$ and $\text{TaFe}_{1+x}\text{Te}_3$.¹⁷ Each NbNiTe_3 layer additionally contains two types of tetrahedral voids which, judged by their size, could be filled by 3d-metal atoms: site A is formed by two edge-sharing octahedra and one tetrahedron, while site B is formed by three edge-sharing octahedra. Both types of tetrahedral voids occur in a 1:1 ratio. Occupation of both sites by Ni atoms leads to a (hypothetical) compound of composition NbNi_3Te_3 , whereas a composition of NbNi_2Te_3 results for a compound with only one type of tetrahedral void filled. Finally, if both sites A and B remain unoccupied, the composition is NbNiTe_3 . The latter type of structure is realized in $\text{TaFe}_{1+x}\text{Te}_3$ ¹⁷ and the corresponding niobium phase,¹⁸ while in the $\text{NbNi}_{2.38}\text{Te}_3$ structure the B sites are filled with Ni atoms. Thus, $\text{NbNi}_{2.38}\text{Te}_3$ can be regarded as stuffed variant of $\text{TaFe}_{1+x}\text{Te}_3$. Additional octahedral, tetrahedral, and square-pyramidal vacancies are found in the interlayer region, of which only the latter are partially occupied by 3d-metal atoms. The electronic factors responsible for the partial occupation of these sites are not yet understood. In contrast to the octahedral and tetrahedral voids in the interlayer region the occupation of the square-pyramidal sites leads to various short metal–metal contacts ($d_{\text{Ni}(3)-\text{Ni}(1)} = 2.637(2) \text{ \AA}$ (2×); $d_{\text{Ni}(3)-\text{Ni}(1)} = 2.738(3) \text{ \AA}$ (1×); $d_{\text{Ni}(3)-\text{Nb}} = 2.980(3) \text{ \AA}$ (1×)). Therefore, we conclude that metal–metal bonding is one important reason for the occupation of this site.

Furthermore, numerous short Nb–Ni and Ni–Ni contacts can be found within a $\text{NbNi}_{2.38}\text{Te}_3$ slab. Ni(1), which is located at the centers of the cross-hatched tetrahedral sites (Figure 1), has two Nb and up to five (note the statistical occupation of the Ni(3) site) Ni neighbors, while Ni(2), occupying the tetrahedral

(14) Yvon, K.; Jeitschko, W.; Parthé, E. *J. Appl. Crystallogr.* **1977**, *10*, 73.

(15) Sheldrick, G. M. SHELXTL/PC. Siemens Analytical X-Ray Instruments, Madison, WI, 1990.

(16) Ibers, J. A.; Hamilton, W. C., Eds. *International Tables for X-ray Crystallography*, Kynoch: Birmingham, England, 1974, Vol. IV.

(17) Neuhausen, J.; Potthoff, E.; Tremel, W.; Enslin, J.; Gütlisch, P. Z. *Naturforsch.* **1993**, *48B*, 785. Badding, M. E.; Li, J.; DiSalvo, F. J.; Zhou, W.; Edwards, P. P. *J. Solid State Chem.* **1992**, *100*, 313. Liu, S.-X.; Cai, G.-L.; Huang, J.-L. *Acta Crystallogr.* **1993**, *C49*, 4.

(18) Li, J.; McDonnell, S. L.; McCulley, F. J. *Alloys Compd.* **1993**, *197*, 21.

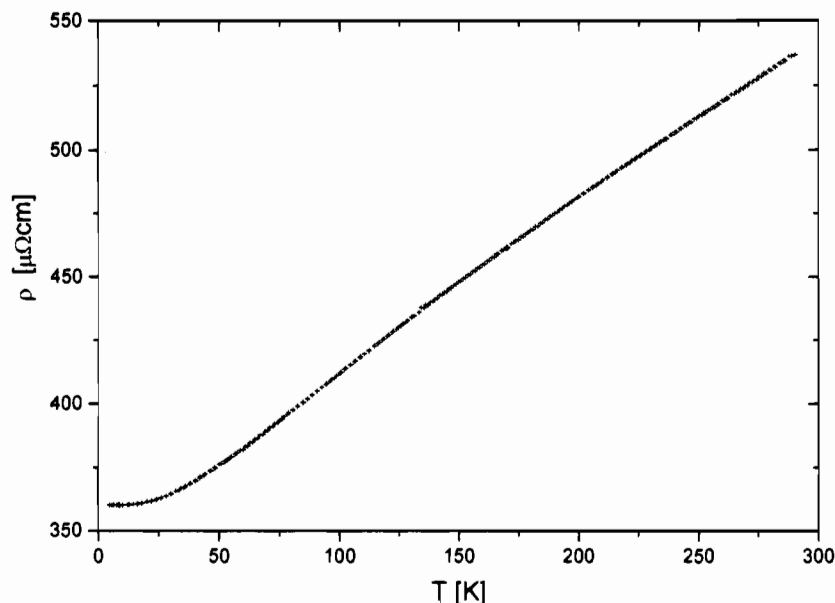


Figure 3. Plot of the specific resistivity as a function of temperature (cooling and heating cycle) of a needle-shaped $\text{NbNi}_{2.38}\text{Te}_3$ -crystal measured along the needle axis.

sites of type *B* (regularly dotted in Figure 1) has three neighboring Nb and two neighboring Ni atoms. Finally, each Nb atom is surrounded by six Ni atoms (for bond distances see Table 3). Compared with the Nb–Ni distances in NbNi_3 ¹⁹ and in ternary early transition metal tellurides such as NbNiTe_2 ²⁰ the corresponding distances in $\text{NbNi}_{2.38}\text{Te}_3$ (approximately 2.7 Å) have to be regarded as strongly bonding. Band structure calculations on these and similar compounds show that metal–metal bonding interactions between early and late transition metals are of crucial importance for the electronic stability of these structures.²¹ The observed Ni–Ni distances (2.57–2.74 Å) are typical for Ni cluster compounds such as $[\text{Ni}_8\text{S}(\text{SC}_4\text{H}_9)_9]^-$ ²² or $[\text{Ni}_4\text{Se}_2(\text{CO})\text{Br}(\text{CpMe})_3]$ ²³ for which significant metal–metal bonding has been discussed. According to the computational results on related compounds²¹ these distances should be considered weakly bonding. The shortest Nb–Nb distance is 3.762(1) Å, while the closest inter- and intralayer Te–Te contacts are 3.740(1) and 3.74(1) Å, respectively. To a first approximation these contacts can be considered non-bonding.

The occupation of type *B* tetrahedral sites formed by Nb_2Te_6 double chains of edge-sharing octahedra results in the formation of rhombuslike Nb_2Ni_2 clusters which are linked via common edges to form a one-dimensional infinite chain. Such $\text{M}_2\text{M}'_2$ clusters ($\text{M} = \text{Nb}, \text{Ta}; \text{M}' = \text{Fe}, \text{Co}, \text{Ni}, \text{Pd}$) are a common structural feature in many metal rich niobium and tantalum tellurides such as $\text{TaM}'_2\text{Te}_2$ ($\text{M}' = \text{Co}, \text{Ni}$)^{21a,b} $\text{MM}'\text{Te}_2$ ($\text{M} =$

$\text{Nb}, \text{Ta}; \text{M}' = \text{Fe}, \text{Co}, \text{Ni}$)^{3,20,21b,c,24} and $\text{Ta}_2\text{M}'_3\text{Te}_5$ ($\text{M}' = \text{Ni}, \text{Pd}$)^{13,21d}. The occurrence of this type of cluster has been related to the electronic stabilization gained by the formation of strong bonds between electron-rich and electron-deficient transition metal atoms.^{21,25} Similar factors are expected to be important for the electronic stability of the $\text{NbNi}_{2.38}\text{Te}_3$ structure as well. Unambiguous assignment of oxidation states for the atoms in $\text{NbNi}_{2.38}\text{Te}_3$ is not possible, but for a metal-rich compound the occurrence of metal atoms in low oxidation states resulting in partially filled d-bands is anticipated. Therefore, $\text{NbNi}_{2.38}\text{Te}_3$ is expected to be a metallic conductor. Indeed, the results of four-probe resistivity measurements (Figure 3) indicate metallic behaviour for $\text{NbNi}_{2.38}\text{Te}_3$ in the temperature range from 5 to 290 K.

In conclusion, ternary niobium and tantalum tellurides can be modified by interstitial atoms on vacant lattice sites of the parent structure. This principle might be extended to other early transition metal chalcogenides with appropriate structural features such as $\text{Ta}_4\text{Pd}_3\text{Te}_{16}$ ²⁶ or $\text{Ta}_4\text{Co}_2\text{PdSe}_{12}$.²⁷ The importance of metal–metal bonding in early transition metal tellurides is confirmed.

Acknowledgment. This work was supported by a grant from the Bundesministerium für Forschung und Technologie under Contract No. 05 5UMGAB and the Fonds der Chemischen Industrie. We are grateful to Heraeus Quarzschmelze (Dr. Höfer) and H. C. Starck Company (Dr. Peters) for gifts of silica tubes and niobium powder, respectively. This work is part of the planned Ph.D. theses of J.N. and E.W.F.

Supplementary Material Available: Tables of crystallographic data, atomic coordinates, anisotropic thermal parameters, interatomic distances and angles (5 pages). Ordering information is given on any current masthead page.

IC950355X

- (19) Pylaeva, E. N.; Gladyshevskii, E. I.; Kripyakevich, P. I. *Zh. Neorg. Khim.* **1958**, *3*, 1622.
 (20) Huang, J.-L.; Liu, S.-X.; Huang, B.-Q. *Sci. Sin.* **B34**, 666.
 (21) (a) Tremel, W. *Angew. Chem.* **1992**, *104*, 230; *Angew. Chem., Int. Ed. Engl.* **1992**, *31*, 217. (b) Tremel, W. *J. Chem. Soc., Chem. Commun.* **1991**, 1405. (c) Neuhausen, J.; Stork, K.-J.; Potthoff, E.; Tremel, W. *Z. Naturforsch.* **1992**, *47B*, 1203. (d) Tremel, W. *Angew. Chem.* **1993**, *105*, 1795; *Angew. Chem., Int. Ed. Engl.* **1993**, *32*, 1752. (e) Li, J.; Hoffmann, R.; Badding, M. E.; DiSalvo, F. J. *Inorg. Chem.* **1990**, *29*, 3943. (f) Rogel, F.; Zhang, J.; Payne, M. W.; Corbett, J. D. *Adv. Chem. Ser.* **1990**, *226*, 369.
 (22) Krüger, T.; Krebs, B.; Henkel, G. *Angew. Chem.* **1989**, *101*, 54; *Angew. Chem., Int. Ed. Engl.* **1989**, *28*, 61.
 (23) Fenske, D.; Hollnagel, A. *Angew. Chem.* **1989**, *101*, 1412; *Angew. Chem., Int. Ed. Engl.* **1989**, *28*, 1390.

- (24) Li, J.; Badding, M. E.; DiSalvo, F. J. *Inorg. Chem.* **1992**, *31*, 1050.
 (25) Brewer, L.; Wengert, P. R. *Metall. Trans.* **1973**, *4*, 83.
 (26) Mar, A.; Ibers, J. A. *J. Chem. Soc.* **1991**, 631.
 (27) Keszler, D. A.; Ibers, J. A.; Shang, M.; Lu, J. *J. Solid State Chem.* **1985**, *57*, 68.